

■ Surface Chemistry

Self-Metalation of Anchored Porphyrins on Atomically Defined Cobalt Oxide Surfaces: In situ Studies by Surface Vibrational Spectroscopy

Tobias Wähler, Ralf Schuster, and Jörg Libuda*^[a]

Abstract: Metalation of anchored porphyrins is essential for their functionality at hybrid interfaces. In this work, we have studied the anchoring and metalation of a functionalized porphyrin derivative, 5-(4-carboxyphenyl)-10,15,20-triphenylporphyrin (MCTPP), on an atomically-defined CoO(100) film under ultrahigh vacuum (UHV) conditions. We follow both the anchoring to the oxide surface and the self-metalation by surface Co^{2+} ions via infrared reflection absorption spectroscopy (IRAS). At 150 K, MCTPP multilayer films adsorb molecularly on CoO(100) without anchoring to the surface. Upon heating to 195 K, the first layer of porphyrin molecules anchors via formation of a bridging surface carboxylate. Above 460 K, the MCTPP multilayer desorbs and only the

anchored monolayer resides on the surface up to temperatures of 600 K approximately. The orientation of anchored MCTPP depends on the surface coverage. At low coverage, the MCTPP adopts a nearly flat-lying geometry, whereas an upright standing film is formed near the multilayer coverage. Self-metalation of MCTPP depends critically on the surface temperature, the coverage and on the molecular orientation. At 150 K, metalation is largely suppressed, while the degree of metalation increases with increasing temperature and reaches a value of around 60% in the first monolayer at 450 K. At lower coverage higher metalation fractions (85% and above) are observed, similar as for increasing temperature.

Introduction

Porphyrins are functional molecules which are at the heart of many emerging technologies.^[1] Because of their unique properties, they are key components in molecular materials and devices, for example in molecular electronics,^[2] chemical sensors,^[3–5] or in photovoltaics.^[6–8] In these applications, the porphyrin units are often attached to interfaces, in many cases to semiconducting oxides.

As far as fundamental studies are concerned, the interaction of porphyrins with surfaces was primarily investigated on metal substrates so far.^[9–18] Surface science studies of porphyrins on metals helped to understand fundamental steps in the adsorption process and, in particular, the metalation reaction. Metalation is among the most critical steps, as the metal ion

incorporated in the porphyrin macrocycle governs the electronic, optical and, chemical properties of the complex.^[9,13,19]

More recently, the interaction of porphyrins with metal oxide surfaces has attracted increased attention, mainly because of the relevance of porphyrin/oxide interfaces in application. In recent studies interfacial reactions of functionalized and non-functionalized tetraphenylporphyrins (TPPs) were investigated on MgO,^[20–24] TiO₂,^[20,25–33] Co₃O₄^[20,34,35] and CoO.^[35] It was shown that the functionalization of the porphyrin molecules and the defect density (steps, corners, edges) play a crucial role in the self-metalation process on MgO nanoparticles.^[22,23] Flat-lying 2HTPP molecules readily metalate via an ion exchange process at room temperature.^[21–23] Functionalized porphyrins however, with one or four carboxylic acid groups, adapt a more upright standing geometry, which suppresses self-metalation.^[21,24] This behavior is also observed for functionalized porphyrins on Co₃O₄ and TiO₂ nanoparticles.^[20] On TiO₂(110), Köbl et al. found protonation of the first layer at room temperature during the adsorption of 2HTPP.^[25] Only at temperatures above 550 K all molecules metalate and form TiOTPP. However, MCTPP is covalently bound to TiO₂(110) with co-adsorbed hydroxyls at room temperature and self-metalation is strongly dependent on the temperature, the coverage and tilting angle of the molecules.^[28] Furthermore, strong dependencies of number and position of the functional acid group on the adsorption geometry on TiO₂(110) were observed.^[26,27,31–33] The authors studied carboxylic acid and phosphonic acid functionalized TPP molecules. The porphyrins carrying only one or two functional groups in *cis* conformation

[a] T. Wähler, R. Schuster, Prof. Dr. J. Libuda
Interface Research and Catalysis
Erlangen Center for Interface Research and Catalysis (ECRC)
Friedrich-Alexander-Universität Erlangen-Nürnberg
Egerlandstraße 3, 91058 Erlangen (Germany)
E-mail: Joerg.Libuda@fau.de

 Supporting information and the ORCID identification number(s) for the author(s) of this article can be found under:
<https://doi.org/10.1002/chem.202001331>.

 © 2020 The Authors. Published by Wiley-VCH GmbH. This is an open access article under the terms of Creative Commons Attribution NonCommercial License, which permits use, distribution and reproduction in any medium, provided the original work is properly cited and is not used for commercial purposes.

are tilted further away from the surface, whereas porphyrins with four anchor groups or two in *trans* conformation bind in a more flat-lying geometry.^[26,27,31–33]

Only few studies were carried out on cobalt oxide surfaces so far. We studied the adsorption of 2HTPP and MCTPP on Co₃O₄(111), which showed clear impact of the functionality on the tilting angles of the molecules at the surface within the monolayer (note that self-metalation was not investigated in this study).^[34] However, self-metalation was observed for non-functionalized 2HTPP on Co₃O₄(111) and CoO(111) at room temperature, very similar to MgO(100).^[35] This work suggests that self-metalation on oxide surfaces is possible, but the reaction is by no means a simple process. So far, the understanding of these interfacial reactions on oxide surfaces is rather limited at the molecular level. In particular, it would be important to explore to what extent the metalation reaction is influenced by the adsorption geometry, coverage, surface temperature or the presence of surface hydroxyl groups at oxide surfaces. In this context, cobalt oxides are of particular interest, as it is possible to prepare thin films of different surface terminations, namely spinel- and rock-salt-type surfaces which introduces the possibility to study these properties in dependency of the surface structure. Both thermodynamic constraints and kinetic barriers are expected to apply, which are more critical than those observed on simple metal surfaces. The studies cited above suggest that anchoring, molecular orientation, and metalation are closely interrelated. In order to better understand self-metalation reactions on oxide surfaces, it is, therefore, essential to perform surface science studies on atomically defined oxides in UHV.

In this work, we applied time-resolved and temperature-programmed infrared reflection absorption spectroscopy (TR-IRAS, TP-IRAS) to monitor both the anchoring reaction and the metalation reaction of a porphyrin on a well-defined cobalt oxide surface. The chemical resolution of IRAS is sufficient to differentiate between free, anchored and metalated porphyrins. Specifically, we used the functionalized porphyrin derivative 5-(4-carboxyphenyl)-10,15,20-triphenylporphyrin (MCTPP) which can bind covalently to an oxide surface via its carboxylic acid functionality (see above). MCTPP was deposited by physical vapor deposition (PVD) onto an atomically-defined CoO(100) thin film prepared on an Ir(100) single crystal. The surface structure of the oxide film has been characterized in detail in previous studies by Heinz, Hammer and co-workers.^[36] The use of thin oxide films instead of single crystals comes with two important advantages. First, the signal intensity of the IR bands is higher than that on bulk oxides and comparable to those on metal surfaces.^[37,38] Secondly, the metal surface selection rule (MSSR) holds strictly for few nanometer thick oxide films on metal single crystals, allowing us to determine the molecular orientation in a straightforward fashion.^[34,39] In this work, we monitor the molecular orientation, the anchoring, and the metalation as a function of coverage of MCTPP and temperature by TR-IRAS and TP-IRAS. We show that there is facile metalation even on a well-ordered oxide surface, however, the reaction depends critically on the surface temperature, the tilting angle and coverage of the porphyrin.

Results and Discussion

In this work, our primary aim is to differentiate by surface IR spectroscopy between the free based porphyrin 5-(4-carboxyphenyl)-10,15,20-triphenylporphyrin (MCTPP) and its metalated counterpart 5-(4-carboxyphenyl)-10,15,20-triphenylporphyrin cobalt(II) (CoMCTPP). To pinpoint the differences in the IR spectra of both species, we compared the bulk IR spectra of MCTPP and its metalated analogue. In Figure 1, we compare IR spectra of the two bulk compounds recorded by attenuated total reflection (ATR) FTIR measurements at 300 K. Characteristic differences are observed, which allow us to identify the metalated and non-metalated species. The detailed assignment of the bands is discussed below. In addition, we show the IRAS data for multilayers of MCTPP and CoMCTPP recorded after PVD at 150 K onto CoO(100). Comparison between the ATR-FTIR and IRAS spectra shows that the bands are identical (apart from differences in intensity which arise from preferred orientation and the MSSR). We conclude that both MCTPP and CoMCTPP can be deposited by PVD without any indication of decomposition.

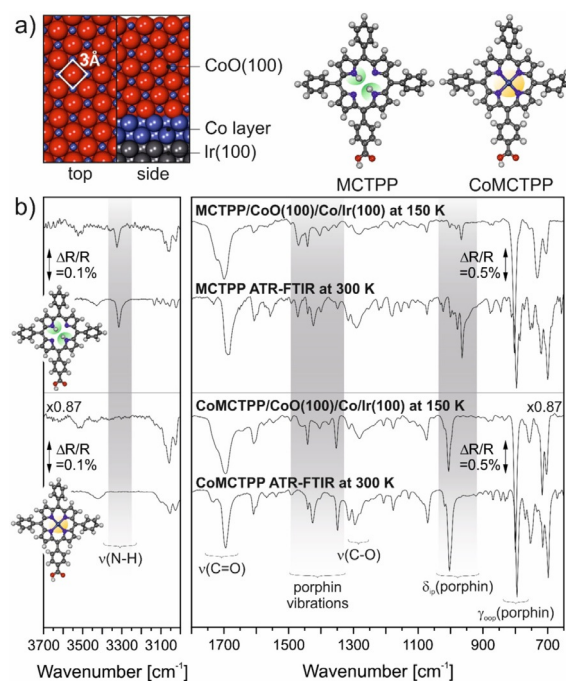


Figure 1. a) Top and side view of CoO(100) film on Ir(100) (left) and chemical structure of MCTPP and CoMCTPP (right). Hydrogen atoms at the free-base MCTPP are marked in green and the Co²⁺ cation incorporated in the macrocycle of the CoMCTPP is marked in yellow. b) Comparison of IRAS spectra acquired at 150 K and the ATR-FTIR spectra of MCTPP and CoMCTPP.

Characteristic vibrations of MCTPP and CoMCTPP

Recently, we studied anchoring of MCTPP on Co₃O₄(111) and compared the IRAS spectra with gas phase IR spectra calculated by density functional theory (DFT).^[34] Following this work and the literature,^[40–42] we assigned the vibrational bands and visualized the corresponding modes using the QVibplot soft-

ware.^[43] Details are given in Table S1 in the Supporting Information. Furthermore, we added the time-resolved spectra recorded during uptake of MCTPP and CoMCTPP at 150 K in Figure S1 (Supporting Information). In this work, we will mainly focus on three aspects: (i) The anchoring of MCTPP on the cobalt oxide surface, (ii) the orientation of the porphyrin molecules with respect to the surface, and (iii) metalation of the porphyrin center of MCTPP induced by Co^{2+} ions released from the surface.

In Figure 1b, we compare IRAS of the multilayer and bulk ATR-FTIR spectra for both MCTPP and CoMCTPP. Spectral regions are highlighted which are of special interest for the following discussion. As mentioned above, IRAS and ATR-FTIR spectra of the compounds are almost identical, indicating that the two compounds can be deposited by PVD without decomposition. All peaks observable are attributed to molecular MCTPP and CoMCTPP, as summarized in the Supporting Information (Table S1). Briefly, both molecules show out-of-plane deformation modes of the porphyrin center ($\gamma_{\text{oop}}(\text{porphyrin})$) at 794–802 cm^{-1} . In the region from 964 to 1005 cm^{-1} , the bands are assigned to in-plane C-N deformation modes within the porphyrin ring ($\delta_{\text{ip}}(\text{porphyrin})$). Between 1348 and 1473 cm^{-1} various vibrational modes are observed, which correspond to skeleton vibrations of the macrocycle. Furthermore, we observe a broad feature at 1277–1296 cm^{-1} and an even more intense band at 1687–1700 cm^{-1} with a shoulder at 1720–1734 cm^{-1} . These features are indicative of an intact carboxyl group and are assigned to the $\nu(\text{C}-\text{O})$ and $\nu(\text{C}=\text{O})$ modes, respectively. In comparison to CoMCTPP, the free-base porphyrin additionally possesses two hydrogen atoms bound to nitrogen atoms in the center of the porphyrin macrocycle. The corresponding $\nu(\text{N}-\text{H})$ modes give rise to a band at 3310–3320 cm^{-1} .

Anchoring of MCTPP to CoO(100)

In the next step, we investigate the adsorption of MCTPP on CoO(100) under isothermal conditions at 300 and 450 K. Werner et al. observed anchoring of MCTPP on $\text{Co}_3\text{O}_4(111)$ at elevated temperatures via the formation of surface bound chelating carboxylates.^[34] Here, we study MCTPP on CoO(100), which is also terminated by Co^{2+} and O^{2-} ions, but differs with respect to the coordination environment and density.^[36] Specifically, the density of surface Co^{2+} ions is higher on CoO(100) and, as a result, the carboxylate function can anchor in form of a bridging carboxylate, the most stable adsorption geometry.^[44]

In Figure 2a, we depict IRAS data recorded during PVD of MCTPP at a sample temperature of 300 K. In addition, we show the intensity of selected bands as a function of coverage. The determination of surface coverage and the complete set of time-resolved IR spectra (see Figure S1) is provided in the Supporting Information. At low coverages, we observe four dominating bands at 717, 800, 1411 and 1473 cm^{-1} . The band at 800 cm^{-1} is assigned to the $\gamma_{\text{oop}}(\text{porphyrin})$ mode. It grows linearly up to coverages of 0.4 ML, then decreases in intensity with on-going deposition and, finally, increases in intensity again at coverages above 1 ML (Figure 2a). The behavior re-

flects a change in orientation of the porphyrin core as a function of coverage and will be analyzed in detail below.

At coverages above 0.4 ML, additional bands are observed at 966, 980, 1001, 1073, 1603 and 3065 cm^{-1} . Here, the $\delta_{\text{ip}}(\text{porphyrin})$ mode at 966 cm^{-1} is the most intense of the three in-plane deformations between 966 and 1001 cm^{-1} . The peak at 1411 cm^{-1} is attributed to $\nu_s(\text{O}-\text{C}-\text{O})$ mode of a surface-anchored carboxylate.^[44–47] However, the antisymmetric stretching mode $\nu_{\text{as}}(\text{O}-\text{C}-\text{O})$, typically exhibiting an absorption band at around 1540 cm^{-1} , is not detectable.^[44,47–50] The absence of this band is explained by the MSSR, which allows detection of perpendicular components of the dynamic dipole moment only.^[39] We conclude that the MCTPP is bound in a bridging geometry. The same adsorption geometry has been proposed for smaller molecules anchored via carboxylic acid groups on CoO(100).^[48,49] Note that the formation of a bridging carboxylate is possible on CoO(100),^[48,49,51] as the $\text{Co}^{2+}-\text{Co}^{2+}$ distance is only 3.0 Å.^[36,52] In contrast, chelating bidentate carboxylates are formed on $\text{Co}_3\text{O}_4(111)$ ^[34] where the $\text{Co}^{2+}-\text{Co}^{2+}$ distance is larger (5.7 Å) and does not permit the formation of a bridging structure.^[36,52] The adsorption geometries for both, bridging and chelating bidentate carboxylates can be found in the Supporting Information (see Figure S3).

Above 1.0 ML, we observe additional bands attributed to multilayer species of MCTPP (see Table S1). In particular, we observe the two bands of the free acid, that is, the $\nu(\text{C}-\text{O})$ band at 1277 cm^{-1} and the $\nu(\text{C}=\text{O})$ band at 1694–1733 cm^{-1} . These bands grow only after saturation of the $\nu_s(\text{O}-\text{C}-\text{O})$ feature, that is, at the point when the porphyrins do not interact directly with the CoO(100) surface anymore.

Next, we investigate the deposition of MCTPP onto CoO(100) at 450 K. The corresponding spectra are shown in Figure 2b. First, we observe that the $\nu(\text{C}-\text{O})$ and $\nu(\text{C}=\text{O})$ band of the free carboxylic acid are absent. This observation indicates that there is only an anchored monolayer of MCTPP present at this temperature. All IR bands observed in this experiment are summarized in Table S1. At coverages below 0.2 ML, we observe only a small peak centered at 715 cm^{-1} , a sharp $\gamma_{\text{oop}}(\text{porphyrin})$ band at 797 cm^{-1} and a broad $\nu_s(\text{O}-\text{C}-\text{O})$ peak at 1399 cm^{-1} , with a prominent shoulder at 1349 cm^{-1} . With increasing coverage, the $\gamma_{\text{oop}}(\text{porphyrin})$ band decreases in intensity and additional IR signals are observed at 964, 1004, 1076, 1599, 3065 and 3310 cm^{-1} . Noteworthy, the $\delta_{\text{ip}}(\text{porphyrin})$ vibration at 1004 cm^{-1} is more prominent than $\delta_{\text{ip}}(\text{porphyrin})$ at 964 cm^{-1} . This observation is in sharp contrast to the isothermal adsorption experiment at 150 K (Figure 1b) and 300 K (Figure 2a).

Previously, we reported that changes in the wavenumber region of $\delta_{\text{ip}}(\text{porphyrin})$ bands are indicative for metalation reactions.^[20] Comparison of the IR spectra of MCTPP and CoMCTPP shows that the metalated complex shows a dominant band at 1002–1005 cm^{-1} whereas the dominant band for the non-metalated complex is located at 964–966 cm^{-1} . Noteworthy, the spectra of MCTPP on CoO(100) acquired at 450 K exhibit also an intense $\delta_{\text{ip}}(\text{porphyrin})$ band at 1004 cm^{-1} . Furthermore, we observe an intense band at 1349 cm^{-1} , which overlaps with the broad $\nu_s(\text{O}-\text{C}-\text{O})$ band (Figure 2b). This feature is also as-

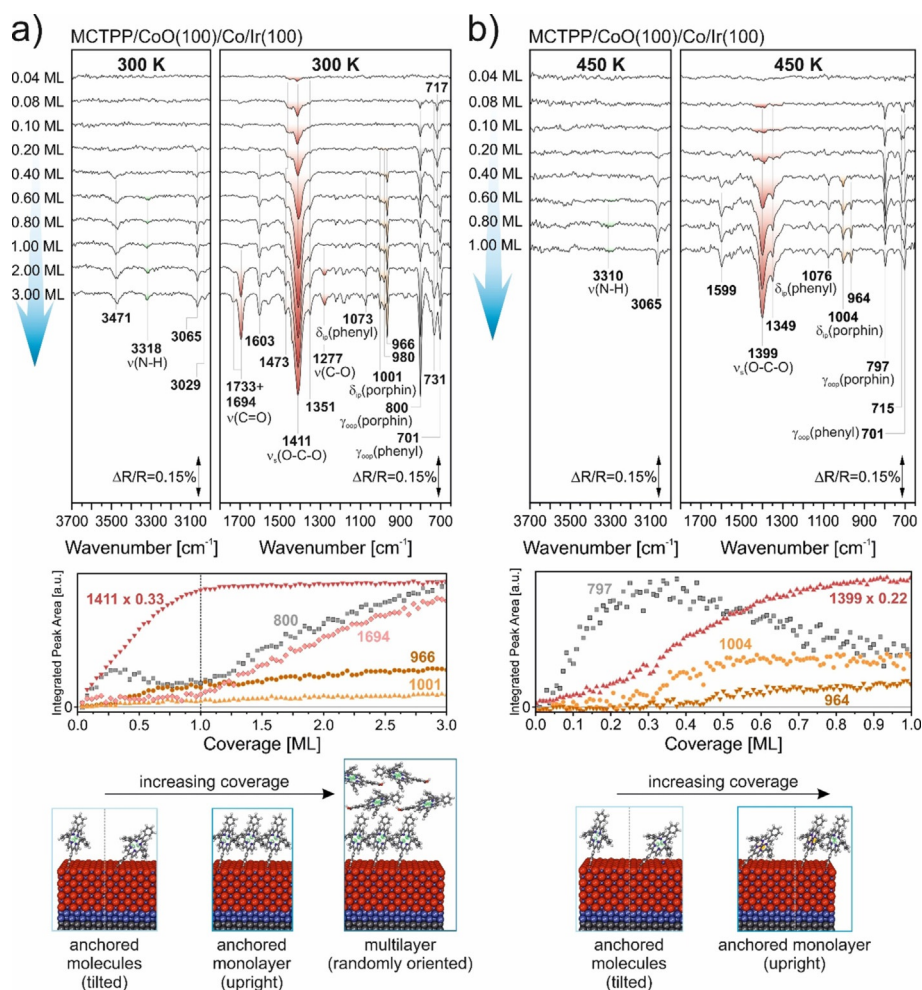


Figure 2. IRAS spectra recorded during the uptake of MCTPP on CoO(100) (a) at 300 K and (b) at 450 K. In the lower panels, we show the integrated peak areas of selected absorption bands and schematic representations of the molecular films.

cribed to the metalated porphyrin. Finally, the ν(N–H) stretching band at 3310 cm⁻¹ is indicative of the free-base porphyrin. In the spectra of MCTPP on CoO(100) acquired at 450 K, the band appears as a very weak and broadened feature only. All these observations suggest that the MCTPP is at least partially metalated to form CoMCTPP upon deposition at 450 K.

Additionally, we can obtain information on the binding motif and adsorption geometry of MCTPP, similar as for deposition at 300 K. Appearance of the strong ν_s(O–C–O) band at 1399 cm⁻¹ indicates the formation of a bridging surface carboxylate. The fact that the intensity of γ_{oop}(porph) is highest at coverages between 0.2 and 0.4 ML and decreases thereafter indicates, once again, reorientation of the anchored porphyrin as a function of coverage (note that the γ_{oop}(porph) mode is polarized perpendicular to the molecular plane). We conclude that MCTPP anchors to the CoO(100) surface in a tilted adsorption geometry at submonolayer coverage, whereas a largely upright standing geometry is adopted upon completion of the monolayer.

Molecular orientation

In order to derive quantitative information on the tilting angle between the molecular plane and the CoO(100) surface, we apply the procedure previously proposed for adsorption of MCTPP on Co₃O₄(111).^[34] A detailed description of the analysis procedure is provided in the Supporting Information. In brief, we calculated the tilting angle α_{ref} from the IR spectrum at a reference coverage of 0.8 ML. All other tilting angles α_t were calculated with respect to this reference value from the most intense γ_{oop}(porph) mode only. The procedure prevents errors due to inaccurate peak integration of very small features (see discussion in ref.^[34]). In Figure 3a, the calculated tilting angle α_t and the integrated peak area of γ_{oop}(porph) are shown as a function of the surface coverage for the adsorption experiments at 300 and 450 K.

For MCTPP adsorption at 450 K and in the limit of small coverage, we find rather large tilting angles between 60°–70° (± 8°), which decrease rapidly to a value of 30°–40° (± 15°) at 0.15 ML. Above this coverage, the tilting angles increase and reach a value of 75° (± 2°) at full monolayer coverage. For MCTPP adsorption at 300 K, the tilting angle could only be de-

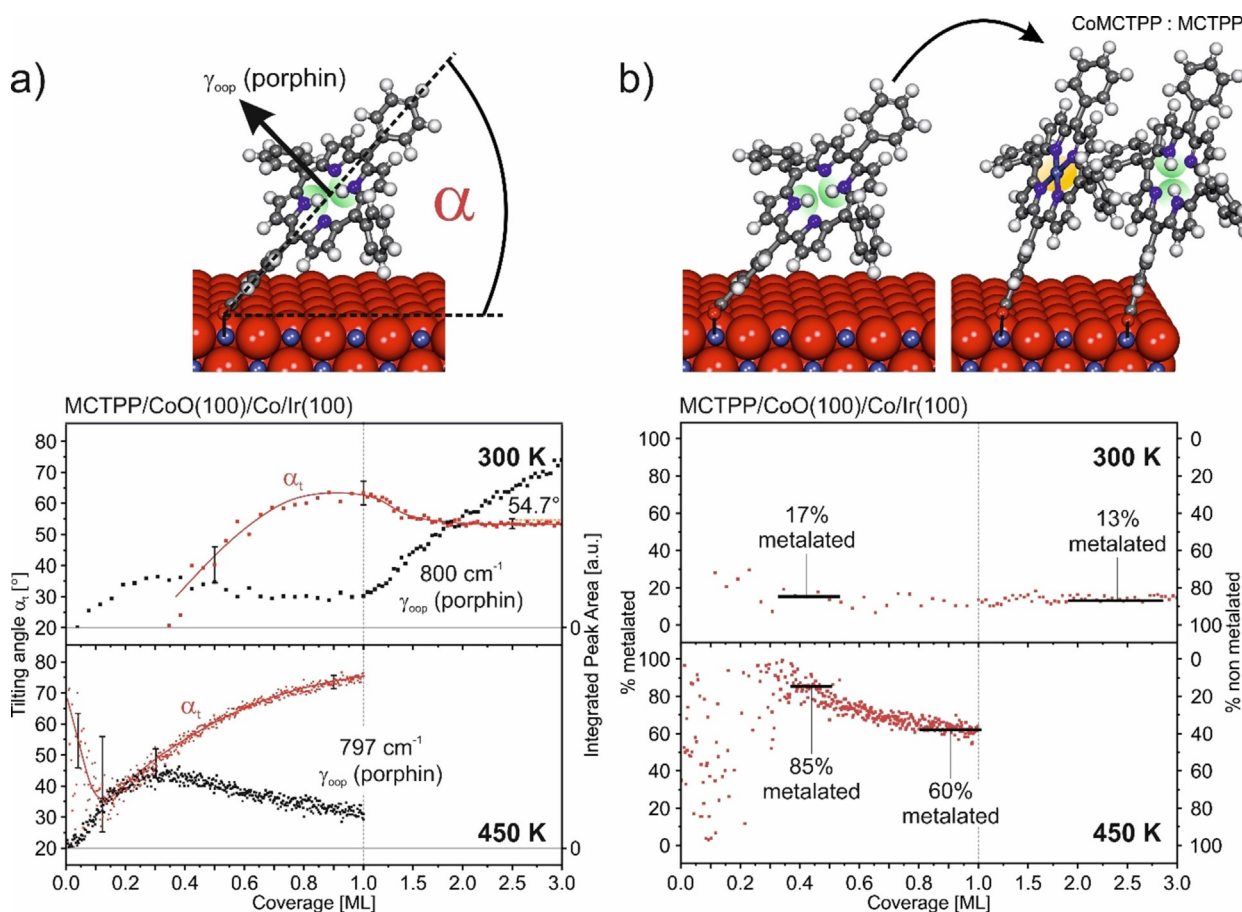


Figure 3. (a) Calculated tilting angles α_t (red) and integrated peak areas of $\gamma_{oop}(\text{porphin})$ (black) as a function of the coverage at 300 and 450 K. (b) Calculated degree of metalation during deposition of MCTPP at 300 and 450 K.

terminated for coverages above 0.15 ML because of the very low intensity and larger width of the bands. Qualitatively, we observe a similar behavior. The tilting angle increases with coverage and reaches a value of $63^\circ (\pm 4^\circ)$ near completion of the monolayer. In the multilayer region, α_t decreases and reaches a value of $53^\circ (\pm 2^\circ)$ at the end of the deposition. This value is close to the magic angle of 54.7° expected for randomly oriented molecules in the multilayer.

Our data suggests that the coverage dependent orientation is similar to what was previously observed for MCTPP on $\text{Co}_3\text{O}_4(111)$.^[34] Here, Werner et al. reported a minimum tilting angle of $25^\circ (\pm 15^\circ)$ at low coverage and a maximum tilting angle of $77^\circ (\pm 5^\circ)$ at monolayer coverage. Similar values were also suggested for MCTPP on $\text{TiO}_2(110)$.^[26] Here, Fernández et al. determined a tilting angle of 66° for MCTPP by Near-Edge X-Ray-Absorption Fine Structure (NEXAFS) measurements of TPP molecules, with different numbers of carboxylic anchor groups.^[26] In summary, the MCTPP tends to lie flat at low coverage and reorients to form a nearly upright standing layer at monolayer coverage. The multilayer grown on top of the first anchored layer is nearly randomly oriented. Noteworthy, the tilting angles in the monolayer grown at 450 K is larger than for the layer grown at 300 K. This observation suggests that the degree of ordering and the packing density increases with

increasing growth temperature. The origin of the larger tilting angles for very small coverages at 450 K is not clear. We propose that the effect is due to adsorption of MCTPP at defects sites of the oxide film. In fact, the CoO film consists of individual grains with deeper boundaries in between. It is likely that some of the initially deposited MCTPP is trapped in these grain boundaries and adopts a larger tilting angle here.

Self-metalation of MCTPP on CoO(100)

To determine the degree of self-metalation in the isothermal adsorption experiments, we used the integrated band intensities of $\delta_{ip}(\text{porphin})$ at $964\text{--}966\text{ cm}^{-1}$ and $1001\text{--}1004\text{ cm}^{-1}$, which are characteristic for MCTPP and CoMCTPP, respectively (see Figure 1b). Details of the evaluation procedure are given in the Supporting Information. Briefly, we calculated the amount of metalated MCTPP using the integrated peak areas of $\delta_{ip}(\text{porphin})$ referenced to the ATR-FTIR spectra of the bulk spectra (to account for the different dynamic dipole moments of the bands). With this approach, we can determine the degree of metalation during the adsorption process from the relative intensity of the $\delta_{ip}(\text{porphin})$ bands at $964\text{--}966\text{ cm}^{-1}$ and $1001\text{--}1004\text{ cm}^{-1}$. The calculated fraction of metalated porphyrin is shown in Figure 3b as a function of surface coverage

for deposition at 300 K and 450 K. For deposition at 300 K, we find that the fraction of metalation is small. Approximately $15 \pm 2\%$ of the porphyrin is metalated and no major changes are observed with increasing coverages. At 450 K, we observe a much higher degree of metalation. Between 0.3 and 0.4 ML, the degree of metalation is approximately 85% and the value decreases to 60% when approaching monolayer coverage. Below 0.3 ML, the intensity of the $\delta_{ip}(\text{porph})$ peak is small and data analysis leads to large uncertainties.

Self-metalation of porphyrins is a well-known phenomenon on various metal surfaces^[14,15,19,53,54] and some oxides.^[22,25,35,55] On metal oxide surfaces, self-metalation typically proceeds via an ion-exchange between the aminic protons and a surface metal cation, often originating from defect sites.^[22,25] Lovat et al., showed that free-base porphyrin molecules deposited on $\text{TiO}_2(110)$ can be protonated by surface hydrogens, most probably from surface hydroxyl groups, which hinders self-metalation.^[56] For adsorption of TPP derivatives on $\text{MgO}(100)$, it was shown that metalation critically depends on the density of defect sites.^[22,23,55] Here, an important point is the stability of the hydroxyl groups formed upon proton release from the porphyrin core. The energetics of the metalation reaction depend on the stability of the OH groups formed upon metalation.

In the present case, Co^{2+} cations must be released from the substrate for metalation, while protons must be taken up. Previously, we studied the formation of surface-hydroxyls upon exposure to water on various thin films ($\text{Co}_3\text{O}_4(111)$,^[57–59] $\text{CoO}(111)$,^[58] $\text{CoO}(100)$,^[58,59] CoO nano-islands^[60]). Drastic differences were observed with respect to the stability of the OH groups. In particular, we did not observe dissociation of water on $\text{CoO}(100)$,^[58,59] suggesting that the stability of OH groups on this surface is comparably low. In a second study, we investigated the anchoring of benzoic acid on different cobalt oxides.^[61] The hydroxyl groups formed upon anchoring, give rise to a sharp $\nu(\text{OH})$ band indicating the formation of isolated hydroxyl groups. In the present study, we did not observe any bands in the wavenumber region from 3600 to 3750 cm^{-1} . This observation suggests that the OH bands are weak and broad and, therefore, difficult to detect. It is likely that the OH groups formed upon deprotonation of the porphyrin center (and possibly also the protons released by the anchoring reaction) are bound at defect sites of the $\text{CoO}(100)$ film. These defects might be present already from the preparation (the film typically grows in form of grains with flat top facets and grain boundaries in between) or their formation may be induced by the metalation reaction. It is likely that also the Co^{2+} ions for the metalation reaction stem from defects such as steps or grain boundaries. After removal of surface Co^{2+} , the same sites may serve as binding centers for the protons.

This scenario is compatible with the observation that self-metalation required elevated temperatures to be activated. We suggest that the anchored MCTPP becomes mobile at elevated temperature and the porphyrin molecules can diffuse to active defect sites on the $\text{CoO}(100)$ film. Wechsler et al. also showed that high surface temperatures are required to increase the degree of metalation for non-anchored 2HTPP both on

$\text{Co}_3\text{O}_4(111)$ and $\text{CoO}(111)$.^[35] The observation suggests that indeed sufficient mobility in the porphyrin film is required. In the present case, anchoring via the carboxylate group further hinders the diffusion. Furthermore, our observations suggest that metalation also depends on the orientation of the molecule with respect to the oxide surface.^[21] Large tilting angles α_t decrease the probability of metalation, simple because of the larger distance between the porphyrin core and the surface, which also leads to a larger activation barrier for metalation. With increasing coverage at 450 K, the tilting angle increases drastically and the tendency for metalation decreases. Previously, Kollhoff et al. has found similar dependencies on the molecular orientation for anchored porphyrins on oxide nanoparticles.^[20,24]

Temperature-induced effects

In order to further investigate the dependence of metalation on the surface temperature, we performed TP-IRAS experiments after isothermal adsorption of MCTPP on $\text{CoO}(100)$ at 150 K. In Figure 4, we show the development of these spectra as a function of temperature and additional peak intensities for selected bands.

For the discussion, we divide the TP-IRAS data into three temperature regimes: (i) 150–195 K, (ii) 195–460 K, and (iii) 460–600 K. In regime (i), the spectra resemble the initial multilayer spectra acquired after deposition at 150 K. In temperature regime (ii), the IRAS spectra change drastically. The intensity of the $\gamma_{oop}(\text{porph})$ and $\nu(\text{C}=\text{O})$ bands decrease with increasing temperatures, whereas the $\delta_{ip}(\text{porph})$ deformation vibrational bands grow in intensity. Furthermore, we observe the formation of the $\nu_3(\text{O}-\text{C}-\text{O})$ band at 1414 cm^{-1} . In regime (iii), finally, the $\gamma_{oop}(\text{porph})$, $\nu(\text{C}=\text{O})$ and $\nu(\text{N}-\text{H})$ bands are completely absent. However, we still observe the $\nu_3(\text{O}-\text{C}-\text{O})$ band of a carboxylate and different band intensities in the $\delta_{ip}(\text{porph})$ region. In particular, the band at 1001 cm^{-1} becomes more prominent and the band at 966 cm^{-1} decreases in intensity.

The development of the $\nu_3(\text{O}-\text{C}-\text{O})$ band during sample heating allows us to follow the anchoring of the MCTPP layer with increasing temperature. Previously, a strong temperature dependence of the anchoring reaction was also observed for MCTPP on $\text{Co}_3\text{O}_4(111)$ ^[34] and ZnDCPP on $\text{TiO}_2(110)$.^[32] The isothermal experiments at 300 and 450 K, further suggest that a reorientation of the porphyrins takes place in the first layer concomitant with the anchoring reaction. Interestingly, the intense $\nu_3(\text{O}-\text{C}-\text{O})$ band is observable over a wide temperature range from 200 to almost 600 K, indicating formation of an anchored layer with high stability. In addition to the $\nu_3(\text{O}-\text{C}-\text{O})$ band, we also observe the $\nu(\text{C}=\text{O})$ stretching mode of the free acid up to 460 K. This suggests that layers of physisorbed MCTPP coexist on top of the anchored monolayer. The multilayer desorbs at 460 K and the monolayer resides up to almost 600 K.

In order to determine the degree of metalation during the TP-IRAS experiment, we apply the same procedure as described above. The results are shown in the inset of Figure 4. Interestingly, we observe a first metalation step in the multilayer-

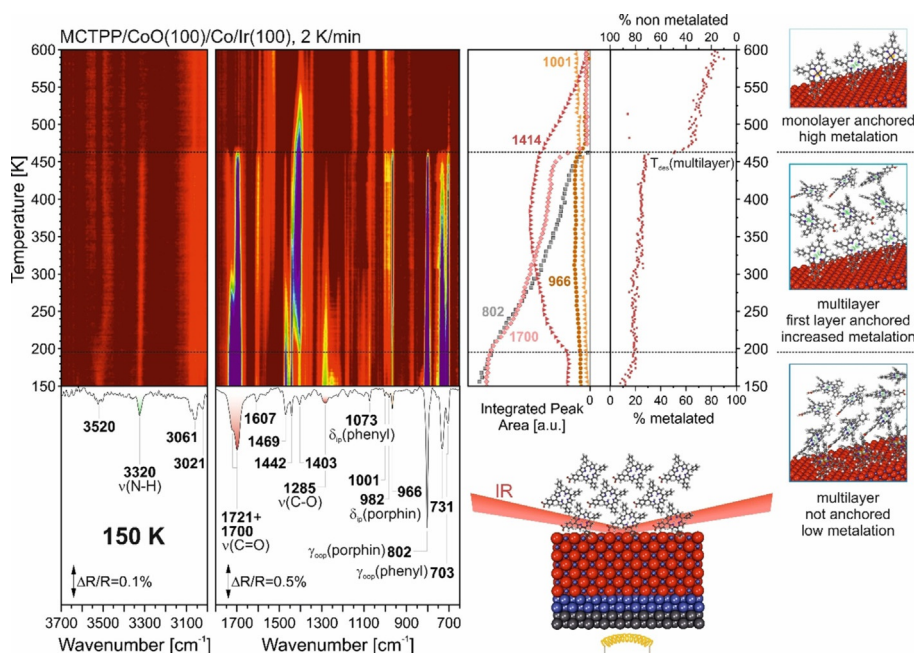


Figure 4. Temperature-programmed IRAS data recorded between 150 and 600 K. The heating rate was 2 K min⁻¹. In the panel on the right, we display integrated peak areas of selected absorption bands. In addition, we calculated the degree of metalation throughout sample heating (see text for details). The schematic representations illustrate the experimental setup and the behavior in different temperature regimes.

er film between 150 and 195 K from 10 to 20%. This degree of metalation increases only slightly to 28% upon heating to 460 K. Upon desorption of the multilayer, the fraction of metalated porphyrins increases and reaches a final value of 80% at 600 K.

Noteworthy are previous XPS studies with non-functionalized 2HTPP, which showed that metalation is possible at low-temperatures on CoO(111).^[35] Here it was found that in the submonolayer region 61% of 2HTPP were already metalated at 175 K. Based on these findings, we propose that a small fraction of the MCTPP multilayer film undergoes metalation already upon deposition at 150 K. However, metalation remains restricted to a minor fraction of molecules in the first monolayer. The low intensity of the carboxylate band at 1403 cm⁻¹ indicates that the majority of MCTPP molecules are not anchored to the surface in this temperature region. It is likely that metalation first occurs for flat-lying molecules, which are in direct contact with defect sites. At 195 K, the first layer of MCTPP anchors to the surface, forming a densely packed layer of upright standing molecules. With increasing temperature, this anchored film undergoes only slow metalation. Upon desorption of the multilayer at 460 K, the fraction of metalated molecules increases from 28 to 60%. This value is in good agreement with the isothermal measurement at 450 K (see Figure 3b). This finding shows that metalation occurs practically exclusively in the first monolayer, but not in the multilayer. Above 460 K however, the degree of metalation further increases up to 80% at 600 K. We attribute this effect to the increasing mobility in the film with increasing temperature.

Conclusion

We studied anchoring, orientation and self-metalation of a carboxyl-functionalized porphyrin, that is, 5-(4-carboxyphenyl)-10,15,20-triphenylporphyrin (MCTPP), on a well-ordered CoO(100) thin film. To this end, we applied isothermal time-resolved IRAS and temperature-programmed IRAS. The main findings are summarized in the following:

- (1) Upon deposition at 150 K, MCTPP adsorbs molecularly on CoO(100) without anchoring to the surface. Upon heating of a multilayer of MCTPP to 195 K, the first layer of porphyrin molecules anchors to the surface via formation of a bridging surface-carboxylate.
- (2) The MCTPP multilayer is stable up to 460 K. Above this temperature, the multilayer desorbs and only the anchored monolayer resides at the surface. The monolayer is stable up to 600 K approximately.
- (3) The orientation of the anchored MCTPP monolayer depends on the surface coverage. At low coverage, the tilting angle is small (30–40°, flat lying molecules), but the angle increases with increasing coverage (75°, upright standing molecules). Larger tilting angles at very low coverage are attributed to the adsorption at defect sites.
- (4) Self-metalation of MCTPP on CoO(100) depends on both, surface temperature and coverage. At low temperature (150 K), the degree of metalation in the first layer is small. With increasing temperature, the degree of metalation increases and reaches a value of around 60% at 460 K. Metalation is limited to the first monolayer only and does not occur in the multilayer. With increasing temperature, the

degree of metalation further increases and reaches a value of around 80% at 600 K.

- (5) The degree of self-metalation depends on the coverage. With increasing coverage, the degree of self-metalation decreases from more than 85% at low coverage to 60% for the full monolayer. These findings suggest that the metalation also depends on the molecular orientation of the anchored species.

Experimental Section

Isothermal IRAS measurements: All IRAS measurements were performed in a UHV setup with a base pressure of 1.5×10^{-10} mbar, which is described elsewhere.^[62] The IR spectra were acquired using a Fourier-transform infrared (FTIR) spectrometer (Bruker Vertex 80v), with an external Liquid-Nitrogen-cooled-Mercury-Cadmium-Telluride (LN-MCT) detector, both connected to the UHV chamber via differentially pumped KBr windows. During deposition of the porphyrins, IR spectra were continuously recorded with a spectral resolution of 4 cm^{-1} and an acquisition time of 60 s per spectrum. All IR spectra were referred to a background spectrum (4 cm^{-1} , 10 min) of the clean surface acquired prior to deposition.

Temperature-programmed IRAS measurements: In the TP-IRAS measurements, IR spectra were continuously recorded (4 cm^{-1} , 60 s) during heating of the sample with an applied heating rate of 2 K min^{-1} . The TP-IRAS data was evaluated, applying the procedure proposed by Xu et al., which accounts for signal intensity losses caused by reflectivity decrease of the surface at elevated temperatures.^[49] The spectrum of the as-prepared CoO(100) thin film was used as reference for the corrected TP-IRAS spectra.

Preparation of CoO(100)/Co/Ir(100): CoO(100) thin films were prepared on an Ir(100) single crystal applying a preparation procedure by Heinz and Hammer.^[36] Starting from a clean Ir(100)-(2 × 1)-O surface, the sample was heated to 523 K for 1 min in 1×10^{-7} mbar H_2 (Linde, 5.3), and subsequently, 1 min in UHV, to yield the Ir(100)-(1 × 1) reconstructed surface. Next, a 3.5–4 nm thick layer of metallic Co was deposited onto the Ir surface at 343 K for 5 min. The sample was then cooled to 193 K and Co was reactively deposited in 7×10^{-7} mbar O_2 for 3 min. The amorphous cobalt oxide film was annealed at 373 K for 3 min to achieve an ordered CoO(100) structure. Applying a second reactive deposition step of Co in an O_2 atmosphere (7×10^{-7} mbar) at 223 K for 20 min, yielded a thick (15 nm) CoO(100) film, which was further annealed at 1073 K for 5 min in UHV. The quality of the prepared CoO(100) film was checked via low-energy electron diffraction (LEED), which showed a clear 1×1 pattern.

Physical vapor deposition of porphyrins: The porphyrins were deposited from glass crucibles using home-built thermal evaporators. The evaporators were separated from the UHV chamber by a gate valve, being pumped via a separate bypass-system. To prevent contamination, the porphyrins were preheated to 453 K for 60 min prior to deposition.

Acknowledgements

This project was supported by the Deutsche Forschungsgemeinschaft (DFG) within the Research Unit FOR 1878 *funcOS—Functional Molecular Structures on Complex Oxide Surfaces* (project number 214951840). Further financial support of the

DFG within the Excellence Cluster *Engineering of Advanced Materials* (Bridge Funding) in the framework of the Excellence Initiative is gratefully acknowledged. Open access funding enabled and organized by Projekt DEAL.

Conflict of interest

The authors declare no conflict of interest.

Keywords: infrared Spectroscopy · interfaces · metalation · oxide surfaces · porphyrins

- [1] W. Auwärter, D. Écija, F. Klappenberger, J. V. Barth, *Nat. Chem.* **2015**, *7*, 105–120.
- [2] M. Jurow, A. E. Schuckman, J. D. Batteas, C. M. Drain, *Coord. Chem. Rev.* **2010**, *254*, 2297–2310.
- [3] Y. Sivalingam, G. Magna, A. Catini, E. Martinelli, R. Paolesse, C. Di Natale, *Procedia Eng.* **2012**, *47*, 446–449.
- [4] M. Ekrami, G. Magna, Z. Emam-Djomeh, M. S. Yarmand, R. Paolesse, C. Di Natale, *Sensors* **2018**, *18*, 2279.
- [5] R. A. Timm, M. P. H. Falla, M. F. G. Huila, H. E. M. Peres, F. J. Ramirez-Fernandez, K. Araki, H. E. Toma, *Sens. Actuators B* **2010**, *146*, 61–68.
- [6] M. Urbani, M. Grätzel, M. K. Nazeeruddin, T. Torres, *Chem. Rev.* **2014**, *114*, 12330–12396.
- [7] C. Y. Lee, C. She, N. C. Jeong, J. T. Hupp, *Chem. Commun.* **2010**, *46*, 6090–6092.
- [8] A. Mahmood, J. Y. Hu, B. Xiao, A. Tang, X. Wang, E. Zhou, *J. Mater. Chem. A* **2018**, *6*, 16769–16797.
- [9] J. M. Gottfried, *Surf. Sci. Rep.* **2015**, *70*, 259–379.
- [10] K. Diller, A. C. Papageorgiou, F. Klappenberger, F. Allegretti, J. V. Barth, W. Auwärter, *Chem. Soc. Rev.* **2016**, *45*, 1629–1656.
- [11] M. Schwarz, M. Garnica, D. A. Duncan, A. Pérez Paz, J. Ducke, P. S. Deimel, P. K. Thakur, T. L. Lee, A. Rubio, J. V. Barth, F. Allegretti, W. Auwärter, *J. Phys. Chem. C* **2018**, *122*, 5452–5461.
- [12] J. M. Gottfried, K. Flechtner, A. Kretschmann, T. Lukaszczuk, H. P. Steinrück, *J. Am. Chem. Soc.* **2006**, *128*, 5644–5645.
- [13] T. E. Shubina, H. Marbach, K. Flechtner, A. Kretschmann, N. Jux, F. Buchner, H. P. Steinrück, T. Clark, J. M. Gottfried, *J. Am. Chem. Soc.* **2007**, *129*, 9476–9483.
- [14] S. Ditze, M. Stark, M. Drost, F. Buchner, H. P. Steinrück, H. Marbach, *Angew. Chem. Int. Ed.* **2012**, *51*, 10898–10901; *Angew. Chem.* **2012**, *124*, 11056–11059.
- [15] M. Lepper, J. Köbl, L. Zhang, M. Meusel, H. Hölzel, D. Lungerich, N. Jux, A. de Siero, B. Meyer, H. P. Steinrück, H. Marbach, *Angew. Chem. Int. Ed.* **2018**, *57*, 10074–10079; *Angew. Chem.* **2018**, *130*, 10230–10236.
- [16] W. Auwärter, A. Weber-Bargioni, S. Brink, A. Riemann, A. Schiffrin, M. Ruben, J. V. Barth, *ChemPhysChem* **2007**, *8*, 250–254.
- [17] K. Diller, F. Klappenberger, M. Marschall, K. Hermann, A. Nefedov, C. Wöll, J. V. Barth, *J. Chem. Phys.* **2012**, *136*, 014705.
- [18] F. Buchner, V. Schwald, K. Comanici, H. P. Steinrück, H. Marbach, *ChemPhysChem* **2007**, *8*, 241–243.
- [19] H. Marbach, *Acc. Chem. Res.* **2015**, *48*, 2649–2658.
- [20] F. Kollhoff, J. Schneider, G. Li, S. Barkaoui, W. Shen, T. Berger, O. Diwald, J. Libuda, *Phys. Chem. Chem. Phys.* **2018**, *20*, 24858–24868.
- [21] J. Schneider, F. Kollhoff, T. Schindler, S. Bichlmaier, J. Bernardi, T. Unruh, J. Libuda, T. Berger, O. Diwald, *J. Phys. Chem. C* **2016**, *120*, 26879–26888.
- [22] J. Schneider, M. Franke, M. Gurrath, M. Röckert, T. Berger, J. Bernardi, B. Meyer, H. P. Steinrück, O. Lytken, O. Diwald, *Chem. Eur. J.* **2016**, *22*, 1744–1749.
- [23] J. Schneider, F. Kollhoff, J. Bernardi, A. Kaftan, J. Libuda, T. Berger, M. Laurin, O. Diwald, *ACS Appl. Mater. Interfaces* **2015**, *7*, 22962–22969.
- [24] F. Kollhoff, J. Schneider, T. Berger, O. Diwald, J. Libuda, *ChemPhysChem* **2018**, *19*, 2272–2280.
- [25] J. Köbl, T. Wang, C. Wang, M. Drost, F. Tu, Q. Xu, H. Ju, D. Wechsler, M. Franke, H. Pan, H. Marbach, H. P. Steinrück, J. Zhu, O. Lytken, *Chemistry-Select* **2016**, *1*, 6103–6105.

- [26] C. C. Fernández, D. Wechsler, T. C. R. Rocha, H. P. Steinrück, O. Lytken, F. J. Williams, *Surf. Sci.* **2019**, *689*, 121462.
- [27] C. C. Fernández, D. Wechsler, T. C. R. Rocha, H. P. Steinrück, O. Lytken, F. J. Williams, *J. Phys. Chem. C* **2019**, *123*, 10974–10980.
- [28] D. Wechsler, C. C. Fernández, H. P. Steinrück, O. Lytken, F. J. Williams, *J. Phys. Chem. C* **2018**, *122*, 4480–4487.
- [29] J. S. Prauzner-Bechcicki, L. Zajac, P. Olszowski, R. Jöhr, A. Hinaut, T. Glatzel, B. Such, E. Meyer, M. Szymonski, *Beilstein J. Nanotechnol.* **2016**, *7*, 1642–1653.
- [30] P. Olszowski, L. Zajac, S. Godlewski, B. Such, R. Jöhr, T. Glatzel, E. Meyer, M. Szymonski, *J. Phys. Chem. C* **2015**, *119*, 21561–21566.
- [31] R. Jöhr, A. Hinaut, R. Pawlak, A. Sadeghi, S. Saha, S. Goedecker, B. Such, M. Szymonski, E. Meyer, T. Glatzel, *J. Chem. Phys.* **2015**, *143*, 094202.
- [32] R. Jöhr, A. Hinaut, R. Pawlak, Ł. Zajac, P. Olszowski, B. Such, T. Glatzel, J. Zhang, M. Muntwiler, J. J. Bergkamp, L. M. Mateo, S. Decurtins, S. X. Liu, E. Meyer, *J. Chem. Phys.* **2017**, *146*, 184704.
- [33] S. Rangan, S. Coh, R. A. Bartynski, K. P. Chitre, E. Galoppini, C. Jaye, D. Fischer, *J. Phys. Chem. C* **2012**, *116*, 23921–23930.
- [34] K. Werner, S. Mohr, M. Schwarz, T. Xu, M. Amende, T. Döpfer, A. Görling, J. Libuda, *J. Phys. Chem. Lett.* **2016**, *7*, 555–560.
- [35] D. Wechsler, C. C. Fernández, Q. Tariq, N. Tsud, K. C. Prince, F. J. Williams, H. P. Steinrück, O. Lytken, *Chem. Eur. J.* **2019**, *25*, 13197–13201.
- [36] K. Heinz, L. Hammer, *J. Phys. Condens. Matter* **2013**, *25*, 173001.
- [37] Y. J. Chabal, *Surf. Sci. Rep.* **1988**, *8*, 211–357.
- [38] C. Yang, C. Wöll, *Adv. Phys. X* **2017**, *2*, 373–408.
- [39] F. M. Hoffmann, *Surf. Sci. Rep.* **1983**, *3*, 107–192.
- [40] J. O. Alben, S. S. Choi, A. D. Adler, W. S. Caughey, *Ann. N.Y. Acad. Sci.* **1973**, *206*, 278–295.
- [41] M. Aydin, *Molecules* **2014**, *19*, 20988–21021.
- [42] X. Y. Li, M. Z. Zgierski, *J. Phys. Chem.* **1991**, *95*, 4268–4287.
- [43] M. Laurin, *J. Chem. Educ.* **2013**, *90*, 944–946.
- [44] T. Xu, S. Mohr, M. Amende, M. Laurin, T. Döpfer, A. Görling, J. Libuda, *J. Phys. Chem. C* **2015**, *119*, 26968–26979.
- [45] C. L. Pang, R. Lindsay, G. Thornton, *Chem. Soc. Rev.* **2008**, *37*, 2328–2353.
- [46] A. G. Thomas, K. L. Syres, *Chem. Soc. Rev.* **2012**, *41*, 4207–4217.
- [47] K. D. Dobson, A. J. McQuillan, *Spectrochim. Acta Part A* **2000**, *56*, 557–565.
- [48] T. Xu, M. Schwarz, K. Werner, S. Mohr, M. Amende, J. Libuda, *Chem. Eur. J.* **2016**, *22*, 5384–5396.
- [49] T. Xu, M. Schwarz, K. Werner, S. Mohr, M. Amende, J. Libuda, *Phys. Chem. Chem. Phys.* **2016**, *18*, 10419–10427.
- [50] J. Van Den Brand, O. Blajiev, P. C. J. Beentjes, H. Terryn, J. H. W. De Wit, *Langmuir* **2004**, *20*, 6318–6326.
- [51] T. Xu, T. Waehler, J. Vecchietti, A. Bonivardi, T. Bauer, J. Schwegler, P. S. Schulz, P. Wasserscheid, J. Libuda, *Angew. Chem. Int. Ed.* **2017**, *56*, 9072–9076; *Angew. Chem.* **2017**, *129*, 9200–9204.
- [52] K. Biedermann, M. Gubo, L. Hammer, K. Heinz, *J. Phys. Condens. Matter* **2009**, *21*, 185003–185013.
- [53] M. Röckert, M. Franke, Q. Tariq, D. Lungerich, N. Jux, M. Stark, A. Kaftan, S. Ditzte, H. Marbach, M. Laurin, J. Libuda, H. P. Steinrück, O. Lytken, *J. Phys. Chem. C* **2014**, *118*, 26729–26736.
- [54] A. Goldoni, C. A. Pignedoli, G. Di Santo, C. Castellarin-Cudia, E. Magnano, F. Bondino, A. Verdini, D. Passerone, *ACS Nano* **2012**, *6*, 10800–10807.
- [55] G. Di Filippo, A. Classen, R. Pöschel, T. Fauster, *J. Chem. Phys.* **2017**, *146*, 064702.
- [56] G. Lovat, D. Forrer, M. Abadia, M. Dominguez, M. Casarin, C. Rogero, A. Vittadini, L. Floreano, *Phys. Chem. Chem. Phys.* **2015**, *17*, 30119–30124.
- [57] G. Yan, T. Wähler, R. Schuster, M. Schwarz, C. Hohner, K. Werner, J. Libuda, P. Sautet, *J. Am. Chem. Soc.* **2019**, *141*, 5623–5627.
- [58] M. Schwarz, S. Mohr, C. Hohner, K. Werner, T. Xu, J. Libuda, *J. Phys. Chem. C* **2019**, *123*, 7673–7681.
- [59] M. Schwarz, F. Faisal, S. Mohr, C. Hohner, K. Werner, T. Xu, T. Skála, N. Tsud, K. C. Prince, V. Matolín, Y. Lykhach, J. Libuda, *J. Phys. Chem. Lett.* **2018**, *9*, 2763–2769.
- [60] T. Wähler, C. Hohner, Z. Sun, R. Schuster, J. Rodríguez-Fernández, J. V. Lauritsen, J. Libuda, *J. Mater. Res.* **2019**, *34*, 379–393.
- [61] M. Schwarz, C. Hohner, S. Mohr, J. Libuda, *J. Phys. Chem. C* **2017**, *121*, 28317–28327.
- [62] P. Ferstl, S. Mehl, M. A. Arman, M. Schuler, A. Toghan, B. Laszlo, Y. Lykhach, O. Brummel, E. Lundgren, J. Knudsen, L. Hammer, M. A. Schneider, J. Libuda, *J. Phys. Chem. C* **2015**, *119*, 16688–16699.

Manuscript received: March 18, 2020

Accepted manuscript online: April 25, 2020

Version of record online: September 3, 2020